Application of AVO attributes to fluid discrimination in a modern delta

Antonio C. Buginga Ramos, Anderson L. Pimentel, Luis O. A. Oliveira e João M. P. de Souza, PETROBRAS S/A

Abstract

The methodology described in this paper was applied in a mud-prone prograding modern deltaic area where sandy turbidites can be found in alternate sedimentary sequences together with silts and thick deepwater shales. The turbiditic deposits are characterized by channel complexes, levee/overbank systems and fan bodies.These reservoirs are normally unconsolidated and strongly affected by the presence of hydrocarbons. AVO anomalies associated with these reservoirs are related to changes in the rock compressibility and density, which are strongly affected by changes in lithology and pore fluids.

Discrimination of saturant fluids was attempted by analysis of analogs generated using different hydrocarbon saturations. AVO anomalies in these synthetic seismograms were computed using fluid factor and other AVO attributes. The values found for background deviation were then used to establish threshold levels for the 3D seismic data. Prior to the computation of AVO attributes the seismic data was carefully scaled so as to keep amplitudes in the same levels as the corresponding synthetics. Using the scaled seismic data a number of AVO attributes were computed. P- and S- inversions were used to compute impedance related attributes like the ones related to the product of Lamé parameters times density. The practical aspects of fluid discrimination using different attribute domains were investigated.

Introduction

The deltaic area where the present methodology was applied is characterized by thick deposits of shales, siltstones and clays. Reservoir quality sands were deposited by a system of channels, which are usually associated with levee and overbank deposits. Slumps and debris flow deposits are also found within the channel complexes.

The sands occuring in the area are generally high porosity and have low impedance with respect to the surrounding shales. The typical problem for hydrocarbon prospecting in the area is the identification of sand bodies that could contain hydrocarbons. Fluid prediction is necessary because of economic constraints that make fluid hydrocarbons more attractive than gas in the area. Also, fluid prediction is critical for separating possible pay sands from brine sands. AVO is currently the preferable technology to achieve the goal of fluid prediction. Despite its natural ambiguity, AVO has proven to be highly successful for lithology and fluid prediction in clastic environments. However, because of its high depositional rate, modern deltas are characterized by the presence of unconsolidated high-porosity brine sands and sand reservoirs saturated by biogenic gas. Under this context, seismic amplitude signatures can be quite ambiguous, causing high-risk AVO anomalies. In such cases, the need for well/seismic calibration using rock properties is very important. Another source of AVO pitfalls in modern deltas is the onset of overpressure, which can cause strong changes in the compressibility and Poisson´s ratio of the rocks (Ramos and Toledo, 2003). Identifying the potential problems and sources of AVO pitfalls can guide the interpreter to avoid high-risk prospects.

In this work, we concentrate our attention to the fluid discrimination issue and the usefulness of the different AVO attributes for identification of pay zones.

Methodology and Examples

In order to achieve fluid prediction, seismic analogs have been built using the data of 400 m of Pliocene section from a control well. The Pliocene section of the control well comprises predominantly shales and few sand bodies saturated by water. P- and S-wave velocities and density were used to construct the ray traced synthetic seismograms. The AVO crossplot corresponding to this section is shown in Figure 1. Fluid substitution was performed in this section so that the most significant Pliocene sand layer of the control well had 60% of liquid hydrocarbon in the pores. The AVO crossplot obtained after fluid substituion exhibits a typical class III response, which is shown in Figure 2. Pay sands are indicated by a polygonal outline in the diagram shown in Figure 2. Fluid discrimination between pay and non-pay sands is then proportional to the deviation of the points within the outline to the background trend represented by the cluster of points near the center of the crossplot. This methodology has been extensively used in the oil industry and has become a standard for AVO analysis. However, the intercept (A) versus gradient (B) domain for anomaly identification is not the only possible petrophysical domain that can be computed from the seismic data. Other petrophysical domains can also be used to better characterize anomalies, with the advantage of getting better sensitivity to the presence of hydrocarbons in different geological scenarios (hard rock, low porosity, etc.).

In this paper we investigate the ways to obtain estimates of a series of petrophysical parameters from seismic data. We also compare different petrophysical domains for crossplotting in terms of anomaly discrimination. Figures

3 and 4 give an example of lambda-rho versus mu-rho crossplots (Goodway et. Al., 1997), for the same brine saturated and hydrocarbon saturated cases shown in Figures 1 and 2. It is clear in Figure 4 that the presence of a sand layer with 60% of liquid hydrocarbon creates an overall shift of the corresponding values of the parameters involved towards low values of lambda-rho. Another way to observe fluid discrimination in the reservoir rock is to measure the separation between the anomaly and the background trend in the crossplot of gradient and intercept (Castagna and Swan, 1997). Figure 5 shows the orthogonal deviation from AVO background trend computed for the top of a Pliocene reservoir, using synthetic models that considered different water saturations. The hydrocarbon anomalies for these sands have usually more than three standard deviations from background trend.

Computation of seismically derived petrophysical attributes followed a methodology that attempts to obtain quantitative measures that are directly related to well log derived parameters. The first step is to compute a filtered version of the intercept and gradient attributes from the log data obtained from control wells. The second step is the computation of RMS average of these attributes. Finally, the seismic data is scaled using the RMS average found in step two. The scaled seismic data is then used in the computation of orthogonal deviations from the AVO background trend, and also in the poststack inversion procedure, to obtain impedance dependent parameters. Estimates of lambda-rho and mu-rho (Goodway et Al., 1997) are directly derived from estimates of P-impedance (Ip) and S-impedance (Is), which are computed from acoustic impedance inversions of Rp=A and Rs=(A-B)/2, respectively. The estimation of Ip and S-impedance is made by a recursive scheme followed by addition of the low frequency component of impedance directly derived from interval velocity fields. The estimation of the S-wave velocity field is done through the use of empirically derived Vp-Vs trends and the P-wave velocity field.

Results

The methodology described in the previous section was implemented in a 3D seismic data. The 3D area is characterized by good seismic data quality, which facilitates the interpretation and computation of AVO estimates.

Figure 6 shows the A-section (AVO intercept), the corresponding AVO crossplot for the outline indicated in the section and the anomalies picked in the third quadrant of the crossplot. These anomalies correspond to sand units with more than three standard deviations from background trend and according to the model should correspond to pay zones.

Figure 7 shows the AVO background deviation section, computed in terms of standard deviations. The arrows indicate possible HC-charged sand units with more than three standard deviations from background trend. A thin dotted line separates low-amplitude more chaotic signals from high-amplitude conformable layers, indicating a possible limit of a clay prone channel. Figure 8 shows the lambda-rho section of the same data presented in Figure 7. Low values of lambda-rho indicate reduced compressibility possibly associated to the presence of hydrocarbons in the sand units indicated by arrows. The limit of the clay rich channel is indicated by a thin dotted line. The lamda-rho section apparently shows a better definition of the channel wall, when compared to Figure 7. This fact is related to improved sensibility of this petrophysical estimate to the abrupt truncation of the comformable sand/shale sequence.

The results obtained through the comparison of different attributes (AVO attributes and seismically derived petrophysical estimates) applied to fluid discrimination in young, unconsolidated clastic sediments, indicate that in such cases no additional benefit is obtained from other attribute rather than the orthogonal deviation from background trend. In areas of low-impedance, class III reservoirs, typically saturated by light hydrocarbons (with high API and high RGO), it is apparent that the same conclusion should hold. In such areas, deviations from AVO background trend are usually superior to three standard deviations.

Conclusions

We used a petrophysically-oriented scheme to scale the seismic data, so as to compute AVO attributes with better quantitative significance.

We exploit the use of different AVO attributes and also seismically determined petrophysical parameters like Ip, Is, lambda-rho and mu-rho to problem of fluid discrimination in young, unconsolidated sediments. The results obtained indicate that, in such cases, the deviation from background trend was able to map all the significant anomalies of interest for exploration purposes. No critical information was added by the other attributes and estimates to the fluid discrimination process.

Acknowledgments

We would like to thank PETROBRAS for the permission to publish this work.

References

Castagna, J. P., **and Swan**, H. W., 1997, Principles of AVO crossplotting: The Leading Edge, 16, 337-342.

Goodway, W., **Chen**, T., **and Downtown**, J., 1997, Improved AVO fluid detection and lithology discrimination using Lame's petrophysical parameter, CSEG Recorder, 22, No. 7, 3-5.

Ramos, A. C. B., **and Toledo**, M. A. S., 2003, Induced AVO anomalies from pore pressure effects, Eighth International Congress of Brazilian Geophysical Society.

Rutherford, R. S., **and Williams**, R. H., 1989, Amplitude-versus-offset variation in gas sands: Geophysics, vol 54, p. 680-688.

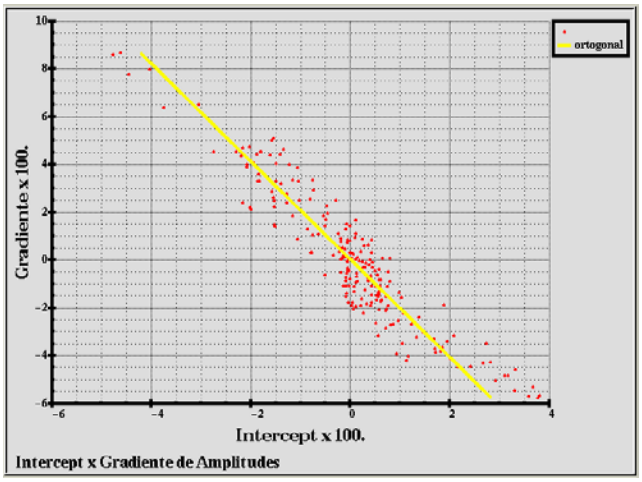

Figure 1 – AVO crossplot of intercept versus gradient for a 400m interval in a typical Pliocene section taken from a control well. The interval shown is comprised by shales and brine sands.

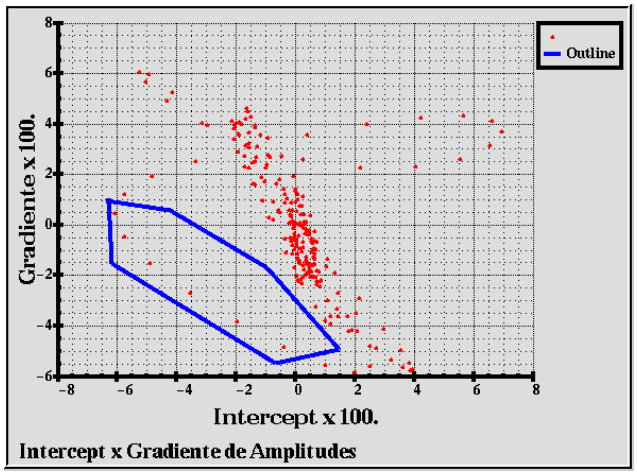

Figure 2 – Same crossplot of Figure 1 after fluid substitution including 60% of oil in a sand reservoir interval.

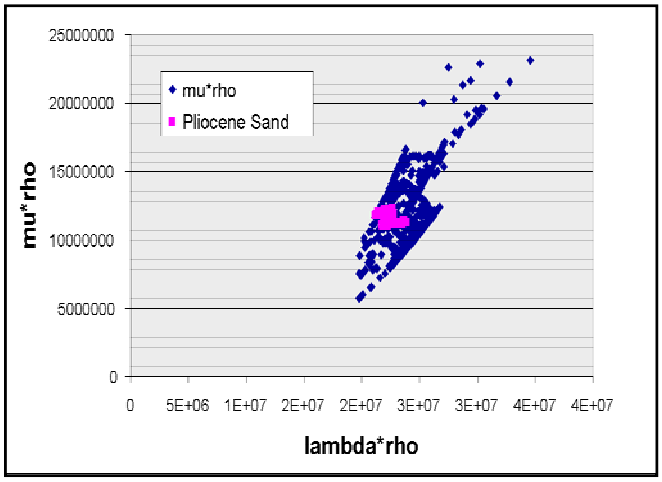

Figure 3 – Crossplot of Lamé parameters times density using the same data shown in Figure 1. Pliocene sands indicated in the figure are 100% water saturated.

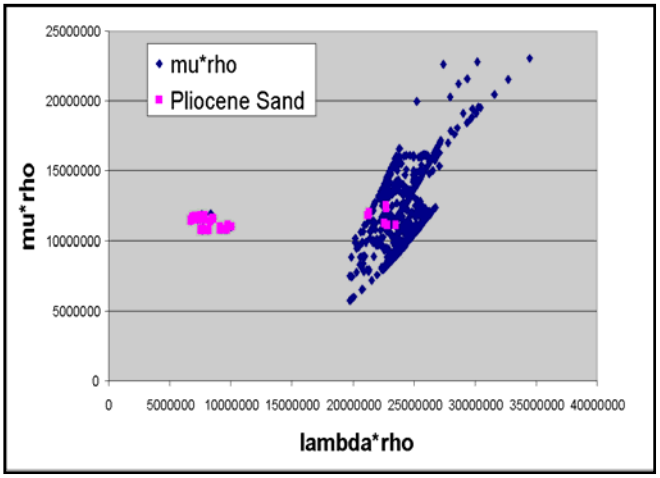

Figure 4 – Crossplot of Lamé parameters times density using the same data shown in Figure 2. Notice the large separation of the sand reservoir in which 60% of oil was introduced replacing water.

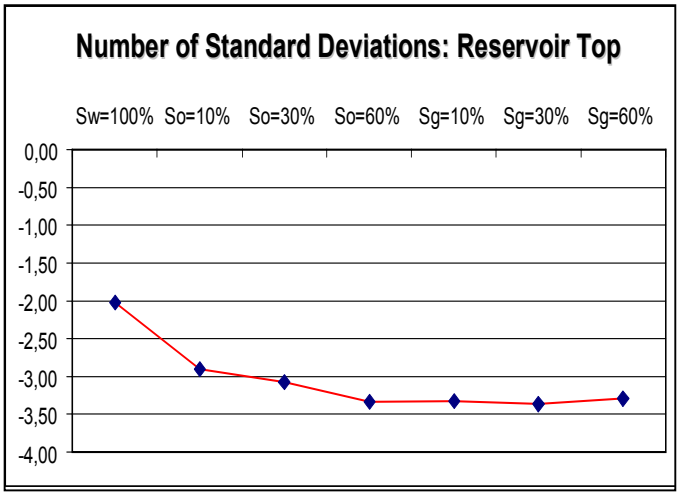

Figure 5 – Orthogonal deviation from AVO background trend computed for models considering different water saturations. Notice that hydrocarbon anomalies have usually more than three standard deviations from background trend.

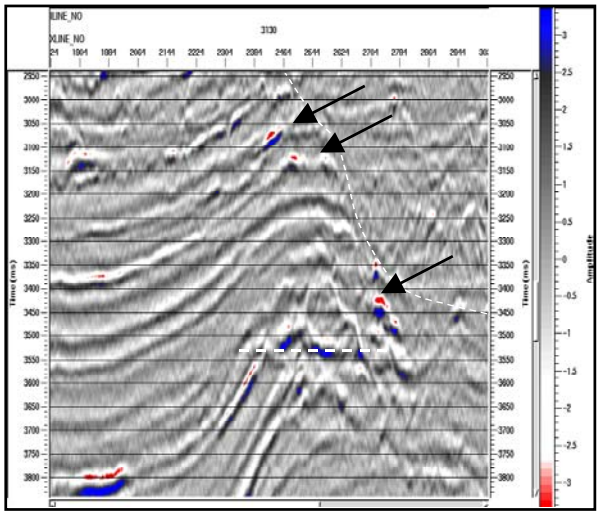

Figure 7 – AVO background deviation section, computed in terms of standard deviations. The arrows indicate possible HC-charged sand units with more than three standard deviations from background trend.

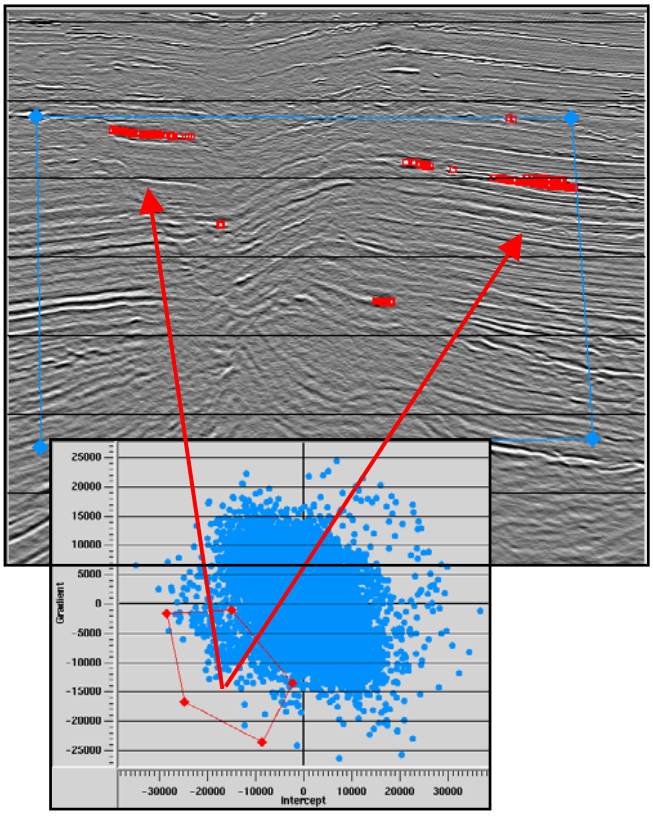

Figure 6 – AVO Intercept section and corresponding AVO crossplot. Notice the strong class III AVO anomalies associated to sand deposits. The number of standard deviations for fluid factor anomaly is above 3 in the selected region of the crossplot.

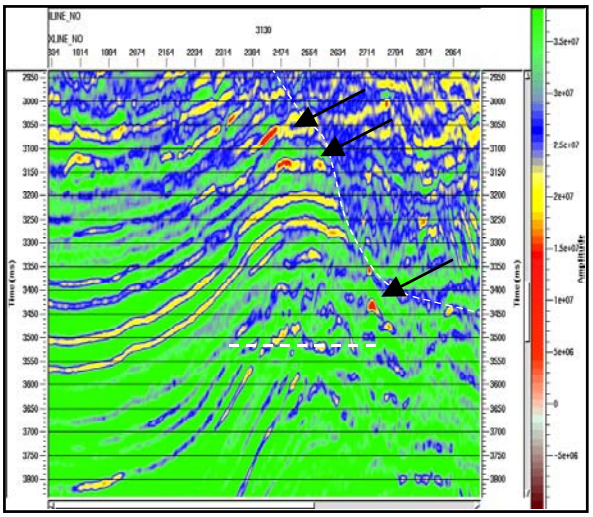

Figure 8 – Lambda-rho section of the same data presented in Figure 7. Low values of lambda-rho indicate reduced compressibility possibly associated to the presence of hydrocarbons in the sand units indicated by arrows.